

tion of iron oxide and affords a high level of control in the synthesis of size-constrained particles.

The synthesized materials are both size- and shape- constrained by the inner volume of the protein cage. Clearly, small molecules have access from the bulk to the interior of the protein cage through pores at the subunit interfaces. However, oxidative hydrolysis selectively entraps the mineral product within the protein cage. This spatial isolation within the protein cage prevents bulk aggregation of the mineral particles and results in a stable, mono-disperse colloid. Our results mimic the reactivity of ferritin-like proteins,<sup>[17,18]</sup> not all of which require the presence of an enzymatic ferroxidase activity for spatially selective mineralization.<sup>[19–21]</sup> Instead, they can rely on a highly charged interior protein interface to induce nucleation. Successful synthetic reactions have utilized electrostatics to nucleate a range of non-native minerals within the ferritin protein cage.<sup>[7–10,22,23]</sup> It has also recently been shown that the native protein cage of lumazine synthase will mineralize iron oxides in a biomimetic synthesis<sup>[24]</sup> analogous to the ferritin system. Our results suggest the potential for re-designing all of these protein cage systems for specific nanomaterials synthesis. Creation of novel chemical environments utilizing the inherent host–guest properties of cage architectures provides a new direction for nanomaterials synthesis.

## Experimental

**Polymerase Chain Reaction (PCR)-Based Site-Directed Mutagenesis:** The mutagenic oligonucleotide primer (5'CAGTCGGAACAGGGGAATTAAC-TGAAGCACAAGAAGAGGCTGCGGCCGAAGAGAACGAGGAGAA-CACGYGTGTGGTCCAACCTG3') and the CCMV coat protein cDNA clone as a template were used to exchange all nine of the N terminal arginine and lysine codons for glutamic acid residues. This mutation in CCMV coat protein gene, termed subE, was confirmed by DNA sequencing.

**Protein Expression:** The mutagenized coat protein gene was expressed in a *Pichia pastoris* heterologous protein expression system (to be described in detail elsewhere [25]). High levels of coat protein expression was induced and yielded assembled viral protein cages devoid of nucleic acid. These protein cages were purified to homogeneity by lysis of cells followed by either chromatography (ion-exchange and/or gel filtration) or by ultra centrifugation.

**Iron Oxide Mineralization:** Solutions of subE (0.5 mg mL<sup>-1</sup>, pH 6.51) were incubated with (NH<sub>4</sub>)<sub>2</sub>Fe(SO<sub>4</sub>)<sub>2</sub>·6H<sub>2</sub>O (25 mM) at room temperature and allowed to air oxidize. Control reactions, protein-free or with an equivalent amount of native CCMV, were performed under identical conditions. Reactions were monitored spectroscopically on a PE lambda 20 UV-vis spectrometer.

**Electron Microscopy:** Transmission electron microscopy data was collected on a Philips CM20 TEM/STEM equipped with Gatan 666 PEELS and EMISPEC Vision system for spectrum imaging.

Received: October 24, 2001  
Final version: January 10, 2002

- [1] S. Mann, F. C. Meldrum, *Adv. Mater.* **1991**, 3, 316.
- [2] S. Mann, D. D. Archibald, J. M. Didymus, T. Douglas, B. R. Heywood, F. C. Meldrum, N. J. Reeves, *Science* **1993**, 261, 1286.
- [3] W. Shenton, D. Pum, U. B. Sleytr, S. Mann, *Nature* **1997**, 389, 585.
- [4] E. Braun, Y. Eichen, U. Sivan, G. Ben-Yoseph, *Nature* **1998**, 391, 775.
- [5] S. R. Whaley, D. S. English, E. L. Hu, P. F. Barbara, A. M. Belcher, *Nature* **2000**, 405, 665.
- [6] G. Xu, I. A. Aksay, J. T. Groves, *J Am Chem. Soc.* **2001**, 123, 2196.
- [7] F. C. Meldrum, V. J. Wade, D. L. Nimmo, B. R. Heywood, S. Mann, *Nature* **1991**, 349, 684.
- [8] F. C. Meldrum, B. R. Heywood, S. Mann, *Science* **1992**, 257, 522.

- [9] T. Douglas, D. P. E. Dickson, S. Betteridge, J. Charnock, C. D. Garner, S. Mann, *Science* **1995**, 269, 54.
- [10] T. Douglas, V. T. Stark, *Inorg. Chem.* **2000**, 39, 1828.
- [11] T. Douglas, M. Young, *Nature* **1998**, 393, 152.
- [12] T. Douglas, M. Young, *Adv. Mater.* **1999**, 11, 679.
- [13] *Biomimetic Materials Chemistry* (Ed: S. Mann), VCH, Weinheim **1996**.
- [14] N. D. Chasteen, P. M. Harrison, *J. Struct. Biol.* **1999**, 126, 182.
- [15] J. A. Speir, S. Munshi, G. Wang, T. S. Baker, J. E. Johnson, *Structure* **1995**, 3, 63.
- [16] Lepidocrocite, (γ-FeOOH) JCPDS file 08–0098.
- [17] P. M. Harrison, P. Arosio, *Biochim. Biophys. Acta* **1996**, 1275, 161.
- [18] M. Bozzi, G. Mignogna, S. Stefanini, D. Barra, C. Longhi, P. Valenti, E. Chiancone, *J. Biol. Chem.* **1997**, 272, 3259.
- [19] D. M. Lawson, P. J. Artymiuk, S. J. Yewdall, J. M. A. Smith, J. C. Livingstone, A. Treffry, A. Luzzago, S. Levi, P. Arosio, G. Cesareni, C. D. Thomas, W. V. Shaw, P. M. Harrison, *Nature* **1991**, 349, 541.
- [20] V. J. Wade, S. Levi, P. Arosio, A. Treffry, P. M. Harrison, S. Mann, *J. Mol. Biol.* **1991**, 221, 1443.
- [21] X. Yang, E. Chiancone, S. Stefanini, A. Ilari, N. D. Chasteen, *Biochem. J.* **2000**, 349, 783.
- [22] F. C. Meldrum, T. Douglas, S. Levi, P. Arosio, S. Mann, *J. Inorg. Biochem.* **1995**, 58, 59.
- [23] T. Douglas, in *Biomimetic Materials Chemistry* (Ed: S. Mann), VCH, Weinheim **1996**.
- [24] W. Shenton, S. Mann, H. Colfen, A. Bacher, M. Fischer, *Angew. Chem. Int. Ed.* **2001**, 40, 442.
- [25] S. Brumfield, D. Willets, T. Douglas, M. Young, unpublished.

## Low-Temperature Fabrication of Light-Emitting Zinc Oxide Micropatterns Using Self-Assembled Monolayers

By Noriko Saito,\* Hajime Haneda, Takashi Sekiguchi, Naoki Ohashi, Isao Sakaguchi, and Kunihito Koumoto

We have succeeded in the low-temperature (55 °C) fabrication of ZnO micropatterns, which show patterned cathodoluminescence images. A photopatterned, self-assembled monolayer (SAM) with phenyl/OH surface functional groups was used as the template. The selective, electroless deposition of ZnO was achieved on a Pd catalyst that had been adhered to the phenyl surfaces only.

ZnO is one of the promising phosphor materials because of its ability to retain a high efficiency, even at low-voltage excitation.<sup>[1]</sup> If micropatterns of it can be produced by a simple process, then the technique for arranging ZnO phosphor should enjoy widespread application, such as in a high-resolution field emission display, which is a new, small-sized flat panel display having higher resolution and better contrast compared to the liquid crystal version. ZnO patterns are also

- [\*] Prof. N. Saito, Dr. H. Haneda, Dr. N. Ohashi, Dr. I. Sakaguchi  
Advanced Materials Laboratory  
National Institute for Materials Science  
1-1 Namiki, Tsukuba, Ibaraki 305-0044 (Japan)  
E-mail: Saito.Noriko@nims.go.jp  
Dr. T. Sekiguchi  
Nanomaterials Laboratory, National Institute for Materials Science  
1-2-1 Sengen, Tsukuba, Ibaraki 305-0047 (Japan)  
Prof. K. Koumoto  
Department of Applied Chemistry  
Graduate School of Engineering, Nagoya University  
Furo-cho, Chikusa-ku, Nagoya 464-8603 (Japan)

applicable to transparent electrodes or surface acoustic wave devices, and their use in integration device technology is greatly anticipated.

In conventional patterning of ceramic thin films, it has been hard to find suitable etching conditions (i.e., conditions that do not influence the substrates used in selective etching), or to obtain high-resolution pattern edges, due to tearing of the ceramic films during the lift-off process. To solve these problems, selective growth techniques have recently been developed. For example, direct patterning is possible by photoenhanced chemical vapor deposition methods.<sup>[2]</sup> Recently, Huang et al. reported a novel synthesis of ZnO nanowires by a vapor transport and condensation process in which the ZnO nanowire was selectively grown onto the Au catalyst particles attached to a surface,<sup>[3]</sup> and they obtained ultraviolet lasing at room temperature (RT).<sup>[4]</sup> However, these growth processes require heat treatments at high temperatures, which can damage substances already present on the substrates. Thus, a new micropatterning technique at low temperature is desirable.

A biomimetic approach for selective deposition using SAM templates<sup>[5–11]</sup> is a versatile technique for such demands. By modifying the surface functional groups of the substrates, interaction with inorganic substances can be controlled and the deposition manner can be designed. We have recently reported the patterning of ZnO on SAMs through the electroless deposition of ZnF(OH).<sup>[11]</sup> The precipitates, however, were not small enough for high-resolution patterning.

Izaki and co-workers<sup>[12,13]</sup> have developed an electroless deposition method for polycrystalline particulate ZnO films through the reduction of nitrate ions using dimethylamine borane. By immersing substrates in an aqueous solution maintained at  $\sim 60^\circ\text{C}$ , crystalline ZnO particulate films were obtained on the Pd catalyst particles attached to the substrates. These conditions proposed for the film formation are thought to be suitable for processing using SAM templates, because SAMs are not stable under severe conditions, i.e., at high temperatures or in high electric fields.

Calvert and co-workers<sup>[14,15]</sup> have extensively investigated the patterning of metals employing SAMs. They showed that Pd/Sn colloids adhered to regions having specific surface properties, such as phenyl terminated surfaces, but not to OH terminated surfaces. Using patterned SAMs as templates, Cu or Ni lines  $\sim 0.4\ \mu\text{m}$  in width were successfully electrolessly metallized along the Pd catalyst attached to the phenyl surfaces.

In the present study, we attempted the micropatterning of ZnO by applying the above mentioned techniques. Figure 1 outlines our strategy for the selective-deposition scheme we employed to fabricate ZnO patterns. A SAM of phenyltrichlorosilane (PTCS) was prepared on a clean Si single crystal substrate ( $<100>$ , p-type,  $15 \times 15 \times 0.5\ \text{mm}^3$ ). The substrate was immersed in an anhydrous toluene solution containing 1 vol.-% PTCS for 5 min, under an  $\text{N}_2$  atmosphere, followed by baking at  $120^\circ\text{C}$  for 5 min in air. The resultant SAM was exposed to UV light through a photomask, for 2 h, in order to pattern the surface with OH and phenyl groups.<sup>[14]</sup> We used

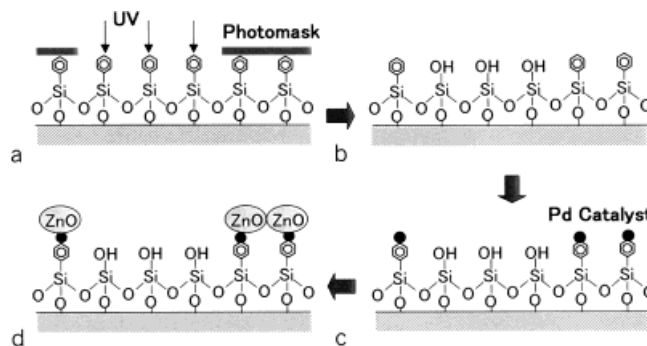


Fig. 1. Schematic diagram of the selective, electroless deposition of ZnO on a phenyltrichlorosilane (PTCS) SAM template. a) A SAM of PTCS is exposed to UV light through a photomask. b) The surface is patterned with OH and phenyl groups. c) The Pd catalyst adheres selectively to the phenyl surfaces. d) ZnO is electrolessly deposited on the Pd attached regions.

the 185 and 254 nm wavelengths of three low-pressure mercury lamps. The irradiance at the sample position (6 cm from the lamps) was about  $3.5\ \text{mW}/\text{cm}^2$ .

Prior to the deposition of ZnO, catalyst particles were selectively attached to the phenyl groups of the substrate. The substrate was initially immersed in an NaCl based Pd/Sn colloid (Cataposit 44, SHIPLEY), which contained  $1.8 \times 10^{-3}\ \text{M}$   $\text{PdCl}_2$  and  $4.2 \times 10^{-2}\ \text{M}$   $\text{SnCl}_2$ , and then in an acidic solution of  $\text{HBF}_4$  (Accelerator 19, SHIPLEY). It is also possible to selectively attach other catalysts, such as when an HCl based colloid (Catalyst 6F, Shipley) or an NaCl based product prepared as described in the patent literature<sup>[16]</sup> is used.

For the electroless deposition of ZnO, the SAM substrate was soaked in an aqueous solution of  $\text{Zn}(\text{NO}_3)_2$  (0.05 M) and dimethylamine borane (DMAB) (0.01 M) at  $55^\circ\text{C}$  for 30 min. The solution of zinc nitrate and DMAB was transparent during the reaction, and hence deposition occurred via heterogeneous nucleation on the Pd catalyst particles attached to the substrate. X-ray diffraction revealed that the deposits were randomly oriented polycrystalline ZnO. The primary crystallite sizes parallel and perpendicular to the  $c$ -axis, estimated from the broadening of the peaks using  $\text{LaB}_6$  as the standard, were about 110 and 40 nm, respectively.

Scanning electron microscopy (SEM) images of the ZnO patterned on the SAM template are shown in Figure 2. The white regions, which correspond to deposited ZnO, indicate an excellent selectivity of deposition—occurring only on the phenyl regions. The ZnO deposits consisted of particles about  $0.2\ \mu\text{m}$  in diameter. The finest line-pattern obtained by this method was  $1\ \mu\text{m}$  wide (Fig. 2b). Ideally, drawing lines as fine as the particle size should be possible by the present deposition method. The edge roughness feature was estimated as several times that of the particle size. The edge acuity was comparable to the recent success with  $\text{TiO}_2$  on a patterned SAM.<sup>[10]</sup> After the surfaces with attached catalyst were fully covered with ZnO (in less than 15 min), no more ZnO particles grew with further soaking, probably because ZnO cannot work as a self-catalyst (as happens in the case of electroless plating of Cu).

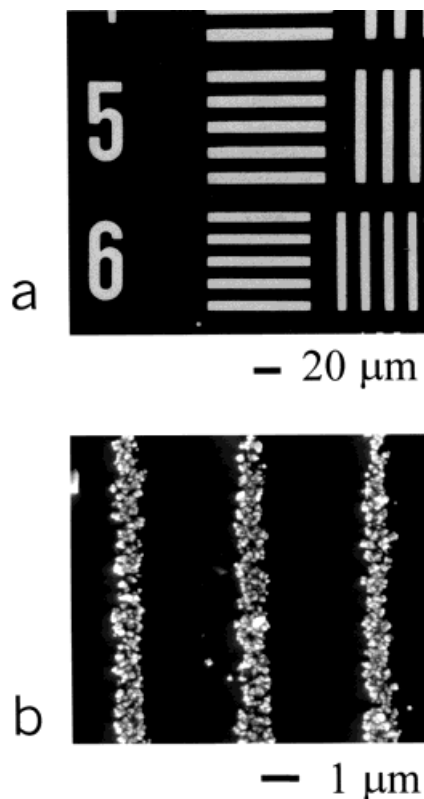


Fig. 2. SEM images of the patterned ZnO. a) Large feature size area and b) 1  $\mu\text{m}$  wide lines. The white regions represent ZnO deposited on the phenyl regions. Particles about 0.2  $\mu\text{m}$  in diameter were deposited.

The surface profilometry of 40  $\mu\text{m}$  wide ZnO lines (measured by Dektak 3030) is shown in Figure 3. The thickness of the particulate film was measured to be about 0.1  $\mu\text{m}$ . Atomic force microscopy measurements gave an estimated standard deviation of the surface roughness (rms) of about 30 nm.

Figure 4 shows a high-resolution transmission electron micrograph (obtained using a JEM-4000EX (JEOL) operated at 400 keV) of ZnO deposited on a Pd catalyst–SAM substrate. The image shows that crystalline ZnO adhered well to the substrate continuously, with an  $\sim 6$  nm thick intermediate amorphous layer of native silicon dioxide and the SAM. At the boundaries between the ZnO particles and the amorphous layer, crystalline catalyst particles, about 3 nm in diameter, were observed.

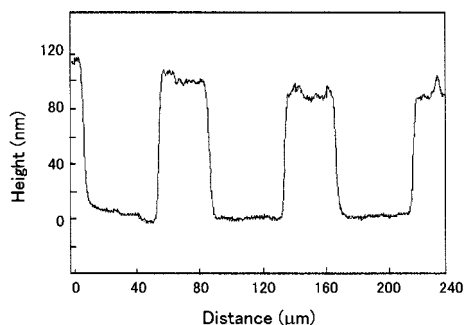


Fig. 3. Surface profilometry of 40  $\mu\text{m}$  wide ZnO lines.

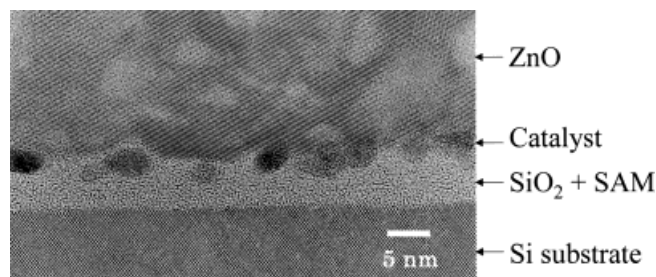


Fig. 4. High-resolution transmission electron micrograph of ZnO deposited on the Pd catalyst–SAM substrate.

Cathodoluminescence (CL) was measured at RT with an electron beam at an excitation voltage of 5 kV and current of 200 pA.<sup>[17]</sup> The spectra measured on the phenyl and OH surfaces are illustrated in Figure 5a. Broad visible light luminescence (500–800 nm) was observed (even without post-annealing) only at the ZnO-deposited regions on the phenyl surfaces. Luminescence of the wavelength longer than that of usual green emission (530 nm) implies that the present sample contained some defects,<sup>[18,19]</sup> which must have been introduced during the deposition carried out under the low-temperature, aqueous conditions. We confirmed that neither the Pd catalyst nor the PTCS SAM showed luminescence.

Figures 5b and c demonstrate monochromatic CL images of 600 nm observed from the same area as shown in Figure 2. The resolution was good enough to obtain virtually the same images as for the SEM images, except that the images looked a little blurred, due to excitation by secondary electrons from neighbors. Figure 5d shows the CL intensity profile along the line indicated in Figure 5b. This suggests that each particulate film of a micropattern is relatively homogeneous, showing only a small fluctuation in luminescence intensity.

In summary, we fabricated a ZnO micropattern by employing a photopatterned PTCS SAM as a template. ZnO was electrolessly deposited selectively on the Pd catalyst attached to the phenyl surfaces. Furthermore, a patterned, monochromatic CL image of visible light was successfully demonstrated for 1  $\mu\text{m}$  wide lines. We believe that the present patterning technique could be used as a low-temperature process for manufacturing light-emitting devices for optoelectronic applications.

Received: October 8, 2001  
Final version: December 12, 2001

- [1] K. Morimoto, in *Phosphor Handbook* (Eds: S. Shionoya, W. M. Yen), CRC Press, Boca Raton, FL **1998**, Ch. 8.
- [2] G. H. Lee, Y. Yamamoto, M. Kourogi, M. Ohtsu, *Thin Solid Films* **2001**, 386, 117.
- [3] M. H. Huang, Y. Wu, H. Feick, N. Tran, E. Weber, P. Yang, *Adv. Mater.* **2001**, 13, 113.
- [4] M. H. Huang, S. Mao, H. Feick, H. Yan, Y. Wu, H. Kind, E. Weber, R. Russo, P. Yang, *Science* **2001**, 292, 1897.
- [5] K. Koumoto, S. Seo, T. Sugiyama, W. J. Dressick, *Chem. Mater.* **1999**, 11, 2305.
- [6] P. G. Clem, N. L. Jeon, R. G. Nuzzo, D. A. Payne, *J. Am. Ceram. Soc.* **1997**, 80, 2821.
- [7] R. J. Collins, H. Shin, M. R. DeGuire, A. H. Heuer, C. N. Sukenik, *Appl. Phys. Lett.* **1996**, 69, 860.
- [8] P. C. Rieke, B. J. Tarasevich, L. L. Wood, M. H. Engelhard, D. R. Baer, G. E. Fryxell, C. M. John, D. A. Laken, M. C. Jaehnig, *Langmuir* **1994**, 10, 619.

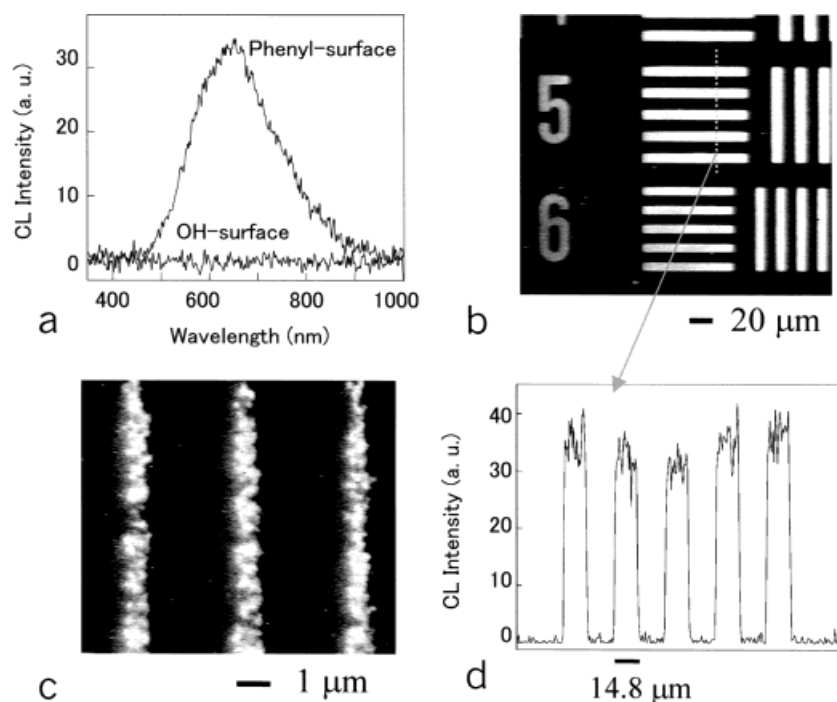


Fig. 5. a) Cathodoluminescence (CL) spectra measured from the phenyl and OH surfaces. Visible light luminescence (500–800 nm) was observed only from the ZnO-deposited phenyl surface regions. b,c) Monochromatic 600 nm CL image for the patterned ZnO: b) large feature size area; c) 1 μm wide lines. These images are virtually the same as the SEM images shown in Figure 2. d) Line profiling of the 600 nm CL intensity along the line indicated in (b).

- [9] B. C. Bunker, P. C. Rieke, B. J. Tarasevich, A. A. Campbell, G. E. Fryxell, G. L. Graff, L. Song, J. Liu, J. W. Virden, G. L. McVay, *Science* **1994**, 264, 48.
- [10] Y. Masuda, W. S. Seo, K. Koumoto, *Langmuir* **2001**, 17, 4876.
- [11] N. Saito, H. Haneda, W. S. Seo, K. Koumoto, *Langmuir* **2001**, 17, 1461.
- [12] M. Izaki, T. Omi, *J. Electrochem. Soc.* **1997**, 144, L3.
- [13] M. Izaki, J. Katayama, *J. Electrochem. Soc.* **2000**, 147, 210.
- [14] J. M. Calvert, M. S. Chen, C. S. Dulcey, J. H. Georger, M. C. Peckerar, J. M. Schnur, P. E. Schoen, *J. Electrochem. Soc.* **1992**, 139, 1967.
- [15] W. J. Dressick, J. M. Calvert, *Jpn. J. Appl. Phys.* **1993**, 32, 5829.
- [16] M. Gulla, W. A. Conlan, *US Patent 3 874 882*, **1975**.
- [17] T. Sekiguchi, *Mater. Res. Soc. Symp. Proc.* **2000**, 588, 75.
- [18] N. Ohashi, T. Nakata, T. Sekiguchi, H. Hosono, M. Mizuguchi, T. Tsurumi, J. Tanaka, H. Haneda, *Jpn. J. Appl. Phys.* **1999**, 38, L113.
- [19] V. V. Osiko, *Opt. Spectra* **1959**, 7, 454.

## Mechanism of the Formation of Self-Organized Microstructures in Soft Functional Materials

By Xiang Yang Liu\* and Prashant D. Sawant\*

Supramolecular functional materials<sup>[1]</sup> continue to attract considerable attention due to their numerous applications in different fields, such as coatings, lithography, biomaterials processing, tissue engineering, textile, paper, packaging, oil fields, and the photography industry.<sup>[2,3]</sup> In order to identify and engineer this type of material, the formation and descrip-

tion of the basic structure of the materials have been a primary goal for many years.<sup>[2]</sup> Supramolecular materials have self-organized three-dimensional (3D) fibrous network structures formed by interconnecting nanosized fibers. It is widely believed that nanofiber networks, which constitute the basic structure of supramolecular materials, are formed via molecular self-assembly.<sup>[1–3]</sup> Apart from this, in the area of colloidal and nanoscale physics, the networks of aggregations are often found to have fractal geometry.<sup>[4–9]</sup> However, there is no report on the identification of fractal characteristics of the networks of supramolecular materials despite the fact that much effort has been devoted to this issue.<sup>[10]</sup>

Here, we report the first in-situ measurement of the formation of fractal fibrous structures in supramolecular functional materials, based on a new rheological and light-scattering method, and a coupled CO<sub>2</sub> supercritical fluid extraction scanning electron microscope (SEM) technique. Instead of self-assembly, a new mechanism, the so-called crystallographic mismatch (or non-crystallographic) branching mechanism that leads to the formation of self-organized network structures, was identified for the first time. It was found that the micro/nanostructure of supramolecular materials will be altered as the experimental condition changes. Such microstructural changes can be characterized by different fractal dimensions. This understanding will allow us to identify robust approaches for the engineering of supramolecular materials.

The nanofibrous network structure to be examined is obtained by dissolving a small molecule gelling agent *N*-laur-oyl-*L*-glutamic acid di-*n*-butylamide (GP-1) (>98 %, from Aijnomoto) in iso-stearyl alcohol (ISA) (>99 %, Cognis), at approximately 125 °C, and lowering the sample temperature

[\*] Prof. X. Y. Liu, Dr. P. D. Sawant  
Interface & Micro/nanostructures Laboratory  
Department of Physics, National University of Singapore  
2 Science Drive3, Singapore 117542 (Singapore)  
E-mail: phyliuxy@nus.edu.sg